

SUPERNOVA RATES: A COSMIC HISTORY

LEV R. YUNGELSON¹ AND MARIO LIVIO

Space Telescope Science Institute, 3700 San Martin Drive, Baltimore, MD 21218

Received 1999 June 21; accepted 1999 July 30

ABSTRACT

We discuss the cosmic history of supernovae on the basis of various assumptions and recent data on the star formation history. We show that supernovae rates as a function of redshift can be used to place significant constraints on progenitor models, on the star formation history, and on the importance of dust obscuration. We demonstrate that it is unlikely that the current observational indications for the existence of a cosmological constant are merely an artifact of the dominance of different progenitor classes at different redshift intervals.

Subject headings: binaries: close — cosmology: observations — stars: formation — supernovae: general

1. INTRODUCTION

The interest in the cosmic history of supernovae stems from several sources. First, core-collapse supernovae (Types II and Ib/c) directly follow the star formation history and some of them may be related to gamma-ray bursts. Second, Type Ia supernovae (SNe Ia) are being used as the primary standard candle sources for the determination of the cosmological parameters Ω and Λ (e.g., Perlmutter et al. 1999; Riess et al. 1998). Third, a comparison of SNe Ia rates (for the different models of their progenitors) with observations may shed light on both the star formation history and on the nature of the progenitors (e.g., Yungelson & Livio 1998; Madau 1998a). Finally, the counts of distant SNe could be used to constrain cosmological parameters (e.g., Ruiz-Lapuente & Canal 1998). As a consequence of the above, studies of cosmological SNe are among the primary targets for the *Next-Generation Space Telescope (NGST)*, which presumably will be able to detect, with proper filters, virtually all the SNe up to a redshift $z \sim 8$.²

In the present study we combine data on the precursors of SNe Ia in our Galaxy with data on the cosmic star formation rate in an attempt to analyze the frequency of events as a function of redshift.

In view of the uncertainties that still exist concerning the cosmic star formation history, we use two types of inputs to characterize the star formation rate (SFR). In the first, we use profiles inferred from deep observations (e.g., Madau, Panagia, & Della Valle 1998). In the second, we use a step-wise SFR that includes a burst of star formation and a subsequent stage of a lower SFR. In the latter case the star formation history is parameterized by the duration of the starburst phase and by the fraction of the total mass of the stellar population that is formed in the burst.

The different scenarios for SNe Ia are briefly discussed in § 2. The basic assumptions and model computations are presented in § 3 and § 4, and a discussion and conclusions follow.

2. THE PROGENITORS OF SUPERNOVAE Ia

The observed SNe Ia do represent somewhat of a mixture of events, with a majority of “normal” ones and a small

minority of “peculiar” ones (see e.g., Branch 1998, and references therein). A more moderate diversity is present even among the “normals.” There exist certain relations between the absolute magnitudes and light-curve decline rates and the morphological types of the host galaxies (e.g., Branch, Romanishin, & Baron 1996; Hamuy et al. 1996). This may suggest a possible diversity among the progenitors of SNe Ia (see, e.g., review by Livio 1999).

On the theoretical side, SNe Ia are very probably thermonuclear disruptions of accreting white dwarfs. Two classes of explosive events are generally considered in the literature. The first involves central ignition of carbon when the accreting white dwarf reaches the Chandrasekhar mass $M_{\text{Ch}} \approx 1.4 M_{\odot}$. In the second, the ignition of the accreted helium layer on top of the white dwarf induces a compression of the core that leads to the ignition of carbon at sub-Chandrasekhar masses (these are known as edge-lit detonations or ELDs). Parameterized models for the events in the former class are able to reproduce most of the typical features of SNe Ia, while ELD models encounter a few serious problems when confronted with observations (see, e.g., Höflich & Khokhlov 1996; Nugent et al. 1997; Branch 1998; Livio 1999 for a discussion and references). On the other hand, binary evolution theory clearly predicts situations in which helium may accumulate on top of white dwarfs (see, e.g., Branch et al. 1995; Yungelson & Tutukov 1997). It is presently not entirely clear whether ELDs indeed do not occur in nature, or whether they are responsible for a subset of the events (e.g., the subluminal ones). However, both the existing diversity in the observed properties of SNe Ia and the uncertainties still involved in theoretical models suggest that it is worthwhile to explore all the possible options.

The occurrence rate of SNe Ia inferred for our Galaxy is $\sim 10^{-3} \text{ yr}^{-1}$ (Cappellaro et al. 1997). There are three evolutionary channels in which, according to population synthesis calculations, the realization frequency of potentially explosive configurations in the disk of the Milky Way is at least at the level of 10^{-4} yr^{-1} . These are the following:

1. Mergers of double degenerates resulting in the formation of a $M \gtrsim M_{\text{Ch}}$ object and central C ignition. The channel involves the accretion of carbon-oxygen.

2. Accretion of helium from a nondegenerate helium-rich companion at a rate of $\dot{M} \sim 10^{-8} M_{\odot} \text{ yr}^{-1}$, resulting in the accumulation of a He layer of $\sim (0.10\text{--}0.15) M_{\odot}$ and an ELD.

¹ Permanent address: Institute of Astronomy of the Russian Academy of Sciences, 48 Pyatnitskaya Street, 10917 Moscow, Russia.

² See <http://ngst.gsfc.nasa.gov/Images/sn.GIF>.

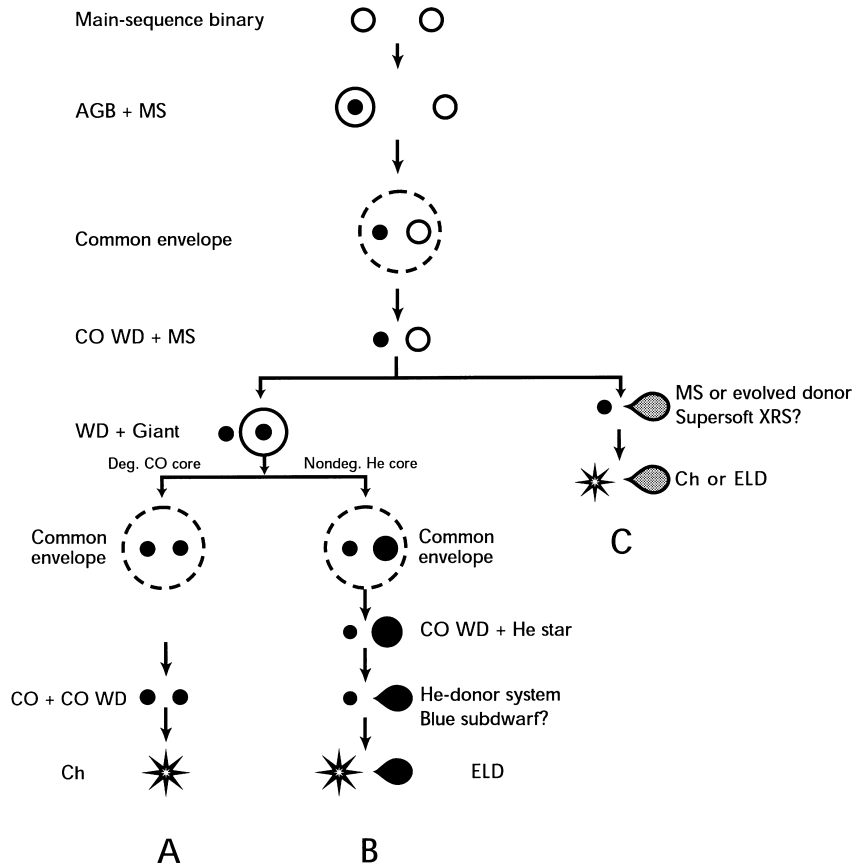


FIG. 1.—Evolutionary scenarios for the most “productive” potential progenitors of SNe Ia. Ch: accumulation of a Chandrasekhar mass by a white dwarf and central carbon ignition. ELD: accumulation of $0.15 M_{\odot}$ of He on top of a sub-Chandrasekhar mass white dwarf. See text for details.

3. Accretion of hydrogen from a (semidetached) main-sequence or evolved companion. The burning of H may result either in the accumulation of M_{Ch} and central C ignition or in the accumulation of a critical layer of He for an ELD.

The positive aspects and drawbacks of these channels were discussed in detail elsewhere and also by other authors (e.g., Tutukov, Yungelson, & Iben 1992; Branch et al. 1995; Iben 1997; Ruiz-Lapuente et al. 1997; Yungelson & Livio 1998; Hachisu, Kato, & Nomoto 1999; Livio 1999). Here we present for “pedagogical” purposes a simplified flow-chart that illustrates some of the evolutionary scenarios that may result in SNe Ia (Fig. 1). Other channels may definitely contribute to the total SNe Ia rate, but they are either less productive or they involve large uncertainties (see also §5).

In a typical scenario, one starts with a main-sequence binary in which the mass of the primary component is in the range $\sim(4-10) M_{\odot}$. The initial system has to be wide enough to allow the primary to become an asymptotic giant branch (AGB) star with a degenerate CO core. After the AGB star overfills its Roche lobe, a common envelope forms. If the components do not merge inside the common envelope, the core of the former primary becomes a CO white dwarf. The subsequent evolution depends on the separation of the components and on the mass of the secondary. If the latter is higher than $\sim 4 M_{\odot}$ and the secondary fills its Roche lobe in the AGB stage, then following a second common envelope phase, a pair of CO white dwarfs forms. The two white dwarfs may merge because of systemic

angular momentum losses via gravitational wave radiation. As a result, a Chandrasekhar mass may be accumulated, leading potentially to a SN Ia (scenario 1).

If the mass of the secondary is above $\sim 2.5 M_{\odot}$ and it fills its Roche lobe before core He ignition it becomes a compact He star. If inside the common envelope the components get sufficiently close, the He star may fill its Roche lobe in the core He burning stage and transfer matter at a rate of $\sim 10^{-8} M_{\odot} \text{ yr}^{-1}$. The accumulation of He on top of the white dwarf may result in an ELD (scenario 2).

Finally, if the mass of the companion to the white dwarf is below $\sim(2-3) M_{\odot}$, the companion may fill its Roche lobe on the main sequence or in the subgiant phase. Such a star could stably transfer matter at a rate that allows for the accumulation of M_{Ch} , or of a critical-mass He layer (scenario 3).

Below we refer to all the potentially explosive situations listed above as “SNe Ia,” in spite of the fact that it is not entirely clear whether most of these configurations actually result in a SN (see, e.g., Livio 1999). We should note that while the above quoted masses are only approximate, the uncertainties are not such that they can change the expected rates significantly.

A special remark has to be made concerning the exclusion of symbiotic stars. Yungelson et al. (1995) have shown that the accumulation of M_{Ch} in these systems occurs at a low rate: $\sim 10^{-5} \text{ yr}^{-1}$ (see, however, discussion in § 5). The accumulation of $0.15 M_{\odot}$ of He via H burning occurs at a rate of $\sim 10^{-4} \text{ yr}^{-1}$, but the accretion rate is typically high, and hence, one would normally not expect an ELD to

ensue. Rather, weak helium flashes may occur. A cautionary note has also to be made concerning ELDs that under certain sets of parameters have an occurrence rate of $\sim 10^{-3} \text{ yr}^{-1}$ in semidetached systems (scenario 3, Yungelson & Livio 1998). We assumed that ELDs occur even if the accretion rate of hydrogen was initially high but then dropped to below $3 \times 10^{-8} M_{\odot} \text{ yr}^{-1}$. By this, we neglected the possible influence of hydrogen flashes on the helium layer. The response of the helium layer and the underlying white dwarf to the varying accretion rate (from several times $10^{-7} M_{\odot} \text{ yr}^{-1}$ to $3 \times 10^{-8} M_{\odot} \text{ yr}^{-1}$) was never treated in detail to the best of our knowledge. One may expect a competition between cooling (due to the expansion of the hydrogen layer) and the inward heat propagation (due to nuclear burning).

Cassisi, Iben, & Tornambè (1998), for example, claim that heating by hydrogen flashes keeps the temperature of the He layer high and may even prevent the explosive ignition of He. Rather, they conclude, quiescent burning may be expected (for accretion rates 10^{-8} to $10^{-6} M_{\odot} \text{ yr}^{-1}$) during which the white dwarf expands to giant dimensions and its envelope may be removed by interaction with the companion. If an explosion nevertheless happens, it may produce a powerful nova-type event (a “super nova”). As a result of all of these uncertainties (and others) the issue of ELDs via a channel of hydrogen accretion is not definitively settled (see Livio 1999).

One of the cornerstones of scenario 3 is the assumption of negligible mass loss in the form of a wind during helium flashes (e.g., Kato, Saio, & Hachisu 1989), which allows for the accumulation of M_{Ch} despite the flashes. The expansion of the helium layers found by Cassisi et al. and the accompanying mass loss may (in some cases at least) prevent the accumulation of M_{Ch} .

Thus, the realization frequency of both scenarios for SNe Ia (explosion at M_{Ch} or at a sub M_{Ch} mass) via channel 3 is a matter of considerable uncertainty. Nevertheless, we include channel 3 in our consideration (although see discussion in § 5).

The basic difference between the possible progenitor scenarios of SNe Ia is in the “evolutionary clock”—the time interval between the formation of the binary system and the SN explosion. Figure 2 shows the dependence of the supernova rate on time after an instantaneous star formation burst, for the four mechanisms listed above, as computed in the present study. The curves shown were computed for a common envelope efficiency parameter $\alpha_{\text{ce}} = 1$; the dependence on this parameter within reasonable limits on α_{ce} between 0.5 and 2 is not too strong. For semidetached systems, we considered the case of mass exchange stabilized by the presence of a thick stellar wind (Hachisu, Kato, & Nomoto 1996; hereafter HKN) as modified by Yungelson and Livio (1998). Further suggested modifications to the standard evolution will be discussed in § 5. The differences in the timespan between the formation of a binary and the SN Ia event, and in the rate of decay of the SNe rates in the different channels, manifests itself in the redshift dependence of the SNe Ia rates.

Our calculations are based on the assumption that the IMF, and the mechanisms of SNe Ia are the same throughout the Hubble time. This assumption may not be valid, for example, because of metallicity effects. Stars with lower Z develop larger helium and carbon-oxygen cores for the same main-sequence mass (e.g., Umeda et al. 1999) and,

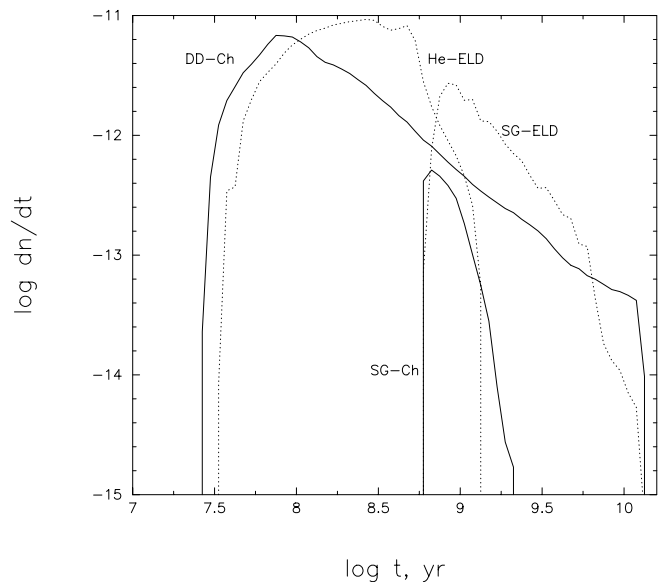


FIG. 2.—Rates of potentially explosive events after an instantaneous star formation burst. The rates are normalized to a formation of $4.7 M_{\odot}$ of stars per year. He-ELD: edge-lit detonations in systems with nondegenerate He donors; DD-Ch: mergers of double degenerates with a total mass above M_{Ch} ; SG-ELD: edge-lit detonations in systems with subgiant donors; SG-Ch: accumulations of M_{Ch} in systems with subgiant donors.

hence, form more massive white dwarfs. At the same time, the upper mass limit of stars that form CO white dwarfs decreases toward a lower metallicity. However, assuming a power-law IMF, both of these effects result in an increased number of potential pre-SNe Ia white dwarfs. On the other hand, a low metallicity can inhibit strong, optically thick stellar winds, which are essential for the HKN model of SNe Ia (Kobayashi et al. 1998). Assuming for the moment that several channels may contribute (see, however, Livio 1999), the net effect may be an enhanced rate of SNe Ia from the channels of double degenerates and ELDs from systems with nondegenerate He donors, and a reduction in the rate from the channel of hydrogen-donor systems.

3. SUPERNOVAE AND THE STAR FORMATION RATE

3.1. Supernovae Rates

The rest-frame frequency of SNe of a certain type at any time t , $n(t)$, may be derived by convolving the star formation rate $\Psi(\tau)$ with the function $f(t)$ giving the rate of SNe after an instantaneous burst of star formation:

$$n(t) = \int_0^t f(t - \tau) \Psi(\tau) d\tau. \quad (1)$$

Two approaches for the evaluation of $f(t)$ are encountered in the literature. The first is not to consider any specific mechanisms of SNe (which are still a matter of some debate), but rather to parameterize f by the fraction of exploding stars in the binary star population (the “explosion efficiency”) and the delay between formation and explosion, or the “evolutionary clock” (e.g., Madau et al. 1998; Dahlén & Fransson 1999; Sadat et al. 1998).

For core-collapse supernovae (SNe II and SNe Ib/c) it is natural to assume that the shape of f follows the SFR and the delay between the formation of the star and the SN event is negligible, since the lifetime of stars more massive than $10 M_{\odot}$ is $\lesssim 20 \text{ Myr}$.

For SNe Ia, Madau et al. considered a parameterized $f(t)$ with timescales of 0.3, 1, and 3 Gyr between the formation of the WD and the explosion. These authors reproduce the ratio of $\text{SN}_{\text{II}}/\text{SN}_{\text{Ia}} \approx 3.5$ in the local universe, if the explosion efficiency is 5%–10%.

A similar parameterization was adopted by Dahln & Fransson (1998), who estimated the number of core collapses and Type Ia SNe that may be detected by *NGST* in different filters for different limiting stellar magnitudes.

Sadat et al. (1998) considered a power law $f \propto t^{-s}$ and explored a range of s from 1.4 to 1.8. Another parameter of Sadat et al. is the rise time of the SNe Ia rate from 0 to a maximum that was fixed at 0.75 Gyr. The ranges of s and rise times were derived from models of the chemical evolution of Fe in elliptical galaxies and in clusters of galaxies. Concerning the explosion efficiency, Sadat et al. actually do not exploit this parameter since they additionally normalize their rates, in order to reproduce the local rate of SNe Ia by the adopted SFR.

A different approach to the determination of f relies on population synthesis calculations. Using this method, Jørgensen et al. (1997) derived the rates of core-collapse supernovae (SNe II and SNe Ib), mergers of binary WDs with a total mass exceeding M_{Ch} , and collapses of Chandrasekhar mass white dwarfs in semidetached systems (in the standard model, without the thick wind of HKN).

Ruiz-Lapuente & Canal (1998; see also Ruiz-Lapuente, Canal, & Burkert 1995; Canal, Ruiz-Lapuente, & Burkert 1996) considered as SNe Ia progenitors merging double degenerates and cataclysmic binaries. For the latter channel, $n(t)$ was estimated in two cases. First, the “standard” case that allows only thermally stable mass exchange for $M_{\text{donor}}/M_{\text{accretor}} \lesssim 0.78$. Second, the case of the “wind” solution of HKN, which allows for mass exchange at rates of up to $\sim 10^{-4} M_{\odot} \text{yr}^{-1}$, for systems with $q \lesssim 1.15$. Ruiz-Lapuente & Canal find a distinct difference between the behavior of the predicted SN Ia rates versus limiting red stellar magnitude for different families of progenitors. Namely, the $dN/dm_R - m_R$ relation for descendants of cataclysmic variables is much steeper than that for merging double degenerates. However, the computations of Dahln & Fransson (1999) do not show any significant difference in the behavior of the SNe Ia counts for different delays in the 0.3–3 Gyr range (the main difference between double degenerates and cataclysmic variable like systems is in the delay time).

3.2. The Star Formation Rate

The star formation rate that is used as an ingredient in calculations of the evolution of the cosmic SNe rate is usually derived from studies that model the observed evolution of the galaxy luminosity density with cosmic time. For example, Madau, Pozzetti, & Dickinson (1998) and Madau, Della Valle, & Panagia (1998; hereafter MDVP98) have shown that the observational data can be fitted if one assumes, as an ingredient of the model, a time-dependent star formation rate. However, there exist uncertainties in this model because of the uncertain amount of dust extinction at early epochs. For example, MDVP98 have shown that the same observational data may be fitted if one assumes a constant $E_{B-V} = 0.1$ or a z -dependent dust extinction that rises rapidly with redshift, $E_{B-V} = 0.011(1+z)^{2.2}$. The latter authors provide convenient fitting formulae for the star formation rates for these two cases.

Model 1 (“little dust extinction”) has

$$\Psi(t) = 0.049t_9^5 e^{-t_9/0.64} + 0.2(1 - e^{-t_9/0.64}) M_{\odot} \text{yr}^{-1} \text{Mpc}^{-3}, \quad (2)$$

where t_9 is the time in Gyr, $t_9 = 13(1+z)^{-3/2}$.

Model 2 (“ z -dependent dust opacity”) has

$$\Psi(t) = 0.336e^{-t_9/1.6} + 0.0074(1 - e^{-t_9/0.64}) + 0.0197t_9^5 e^{-t_9/0.64} M_{\odot} \text{yr}^{-1} \text{Mpc}^{-3}. \quad (3)$$

Note that equations (2) and (3) give slightly different current SFRs, and the integrated values are also different by about 10%. Both SFR models predict a similar, rather steep rise, by a factor ~ 10 , at $z \lesssim 1.5$. The difference between the two rates is in the behavior at $z \gtrsim 1.5$. While in the “little dust extinction” case the rate drops almost linearly by a factor of about 10 to $z_* = 5$, in the “ z -dependent dust opacity” case it continuously grows to z_* , by a factor of ~ 2.5 . Formally, the star formation process switches on discontinuously at z_* .

We should note that model 2 may be a more realistic representation of the global star formation history, since there is growing evidence of a significant effect of dust absorption at high z (e.g., Pettini et al. 1998; Calzetti & Heckman 1999; Huges et al. 1998; Steidel et al. 1999; Blain et al. 1999). Also, selection effects due to the low surface brightness of galaxies (e.g., Ferguson 1998) or the shift of typical spectral features to the red (e.g., Hu, Cowie, & McMahon 1998) may result in an underestimate of the SFR at high redshifts.

Equation (2) gives a star formation history that is consistent with expectations from hierarchical clustering cosmologies, while equation (3) gives the model prediction for SFR typical for a monolithic collapse scenario (e.g., Madau 1998b).

Ruiz-Lapuente & Canal (1998) used in their computations the star formation rate given by Madau (1997), without corrections for dust extinction. The effect of extinction was considered by Dahln & Fransson (1998) and by Sadat et al. (1998). In the latter case, the SFR at $z \gtrsim 1$ was taken to be several times higher than in the “low-dust” case. Jørgensen et al. (1997) considered two modes of star formation: a “burst” lasting for 500 Myr, and a continuous SFR for a Hubble time, and computed models for a range of relative contributions of both star formation modes.

4. MODEL COMPUTATIONS

4.1. Models Using “Observed” Star Formation Rates

The population synthesis code used for the computations of the SNe rates was previously applied by the authors to a number of problems related to the population of Galactic binary stars and, in particular, to SNe. Within the range of observational uncertainties, the code reproduces correctly the rates of SNe inferred for our Galaxy (Tutukov, Yungelson, & Iben 1992; Yungelson & Livio 1998 and references therein).

Throughout this paper we assume a cosmology with $\Omega_0 = 1$, $H_0 = 50 \text{ km s}^{-1} \text{Mpc}^{-1}$. These values of the cosmological parameters are assumed only for convenience. Our qualitative results and conclusions do not depend on this choice. Star formation is assumed to start at $z_* = 5$. The Hubble time in this model was taken to be 13 Gyr.

For the different SNe Ia scenarios listed in § 2 and for different star formation histories, we first calculated the rest-frame rates of events n_0 . We then computed differential functions for the number of events observed at redshift z and cumulative functions $n (< z)$. We use equation (3.3.25) from Zeldovich & Novikov (1983) for the number of events observed from a layer between redshifts z and $z + dz$ in an expanding, curved universe, taking into account time dilation:

$$\frac{dn}{dz} = n_0 \frac{4\pi c^3}{H_0^3} \frac{1}{1+z} \xi_z(z, \Omega_0) z^2 dz, \quad (4)$$

where, for the particular case of $\Omega_0 = 1$,

$$\xi_z(z, 1) = \frac{4[(1+z)^{1/2} - 1]^2}{z^2(1+z)^{5/2}}. \quad (5)$$

Notice, that $\partial \xi_z / \partial z < 0$. Time t is related to z as

$$t = \frac{2H_0^{-1}}{3(1+z)^{3/2}}. \quad (6)$$

We operate with the *number of events per year* instead of expressing the SNe rates in the more conventional supernovae units (SNU), since both the computation of blue luminosities and their observational determination involve additional parameters (expressing the rates in SNU may result in loss of information on both the SNe rates and on the SFR).

Our simulations give the rates of SNe as a function of z . Clearly, the number of observable events depends on other factors such as the limiting stellar magnitude of the sample, etc. Nevertheless, our results provide the basis for theoretical expectations, which need subsequently to be convolved with observational selection effects. In principle, *NGST* observations can approach the theoretical limits. Figure 3 compares the values of dn/dz for the different channels of SNe and the different assumptions about the SFR given by equations (2) and (3). Figure 4 shows the behavior with redshift of the cumulative numbers of SNe.

The behavior of dn/dz can be understood as follows. In model 1 (low dust) as one progresses from $z = 0$ to z_* , the SFR reaches a maximum at $z \approx 1.5$. The maxima of the rest-frame SNe rates happen at a slightly lower z in order of decreasing delay times: ELDs in systems with subgiant companions, M_{Ch} accumulations in the latter, mergers of double degenerates, ELDs in systems with nondegenerate He donors, core-collapse SNe (Fig. 2). The behavior of the dn/dz counts depends also on the geometrical z -dependent factors given by equations (4) and (5). In particular, the derivative of the product $z^2 \xi_z$ changes sign from positive to negative at $z \approx 0.96$. This factor shifts the maximum in the counts to a lower z . The steep rise of dn/dz at low z is entirely the result of the expanding horizon.

Similarly, in Model 2 (z -dependent dust opacity), the behavior of dn/dz at low z is dominated by the expansion of the comoving volume and the rates suggested by the two models are almost indistinguishable. However, already at $z \sim 0.5$, the increase in the rates in Model 2 becomes somewhat less steep, reflecting the more moderate growth of the SFR. The rate of core-collapse SNe starts to decrease at $z \approx 1.2$ despite the continuous growth of the SFR. This is a consequence of the negative $\partial \xi_z / \partial z$. The rates of SNe Ia start to decline at a higher z , as a consequence of the longer delay times. The difference in the time delays between SNe II and the different hypothetical SNe Ia manifests itself in an increase in the SN Ia/SN II ratio at low z and its subsequent decline (Fig. 7). This feature was already noticed by Yungelson & Livio (1998) for SNe Ia from double degenerates, but in the present study we find that (1) this effect is less pronounced because of the different approximation to the SFR and (2) the redshift of the maximum of the ratio is different for different SNe Ia scenarios.

The difference in the rate of decline of dn/dz at $z \gtrsim 1$ is clearly distinct in Models 1 and 2 and may provide important information about the star formation behavior.

The most pronounced feature of dn/dz for both types of dust models is the disappearance of SNe Ia at $z \approx 3$ for the channels of progenitors with relatively long delays. Thus, in

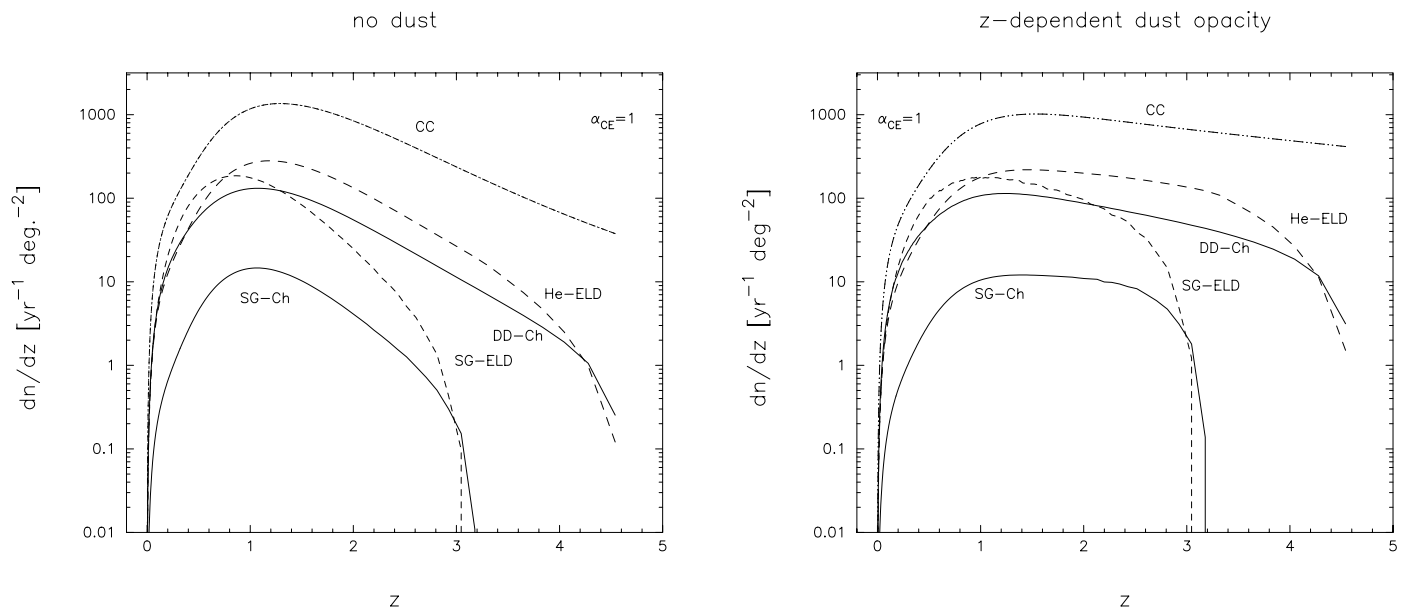


FIG. 3.—Number counts of SNe per unit Δz vs. redshift for different channels of explosive events in models 1 (“low dust”) and 2 (“ z -dependent dust opacity”). Notations as in Fig. 2. CC denotes core-collapse supernovae.

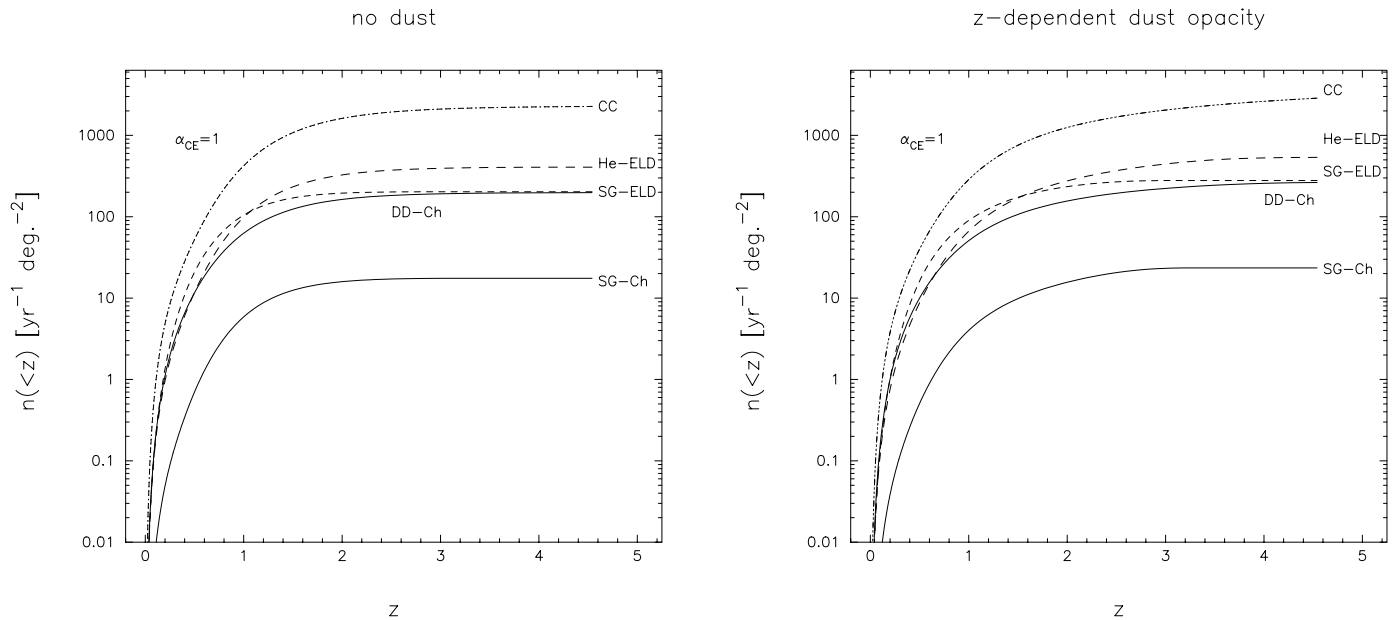


FIG. 4.—Cumulative counts of SNe below a given redshift z for different channels of explosive events in models 1 and 2. Notations as in Figure 2.

principle, a determination of SNe Ia rates at $z \gtrsim 3$ with *NGST* can unambiguously distinguish between different progenitor models. Long delay times are typical for both modes (Chandrasekhar or sub-Chandrasekhar explosions) of SNe Ia resulting from systems with subgiant donors.

The relative role of different channels for SNe Ia changes with z . In both models 1 and 2 (for the dust) mergers of double degenerates dominate over ELDs in systems with He nondegenerate donors up to $z \lesssim 0.4$. In model 1, ELDs in systems with subgiants dominate over He-ELD at $z \lesssim 0.8$ and over DD-Ch at $z \lesssim 1.3$. In model 2 these limits are at about $z \sim 1$ and $z \sim 2.2$. If it were the case that all three channels really contribute to SNe Ia but have somewhat different characteristics, one would expect to find variations in the statistical properties of SNe Ia with redshift. We will return to this point in the discussion.

As expected, the cumulative numbers of SNe grow faster in the “low-dust” case than in the model with dust. Only the cumulative counts of SNe II and SNe Ia from the DD-Ch and He-ELD channels grow continuously to high redshifts, while those for SNe involving subgiants saturate at $z \sim 3$.

To summarize this section: observations of SNe beyond $z \approx 1$ can provide valuable information on the star formation rate (see also § 5). The counts of SNe Ia at $z \gtrsim 3$ will indicate the timescale of the delay between births of binaries and SN events and will then provide information on the nature of the progenitors.

4.2. Parameterized Star Formation Rates

The main uncertainty in the global SFR is a result of the effects of dust obscuration in star-forming galaxies (see, e.g., Calzetti & Heckman 1998 and Pettini et al. 1998 for a discussion of the fraction of light absorbed by dust). Therefore, it is worthwhile to investigate the cosmic history of SNe for several parameterized SFR.

We consider four parameterized modes of galactic star formation (intended to bracket and cover a range of possibilities):

Model 3.—Constant star formation rate from $z_* = 5$ to $z = 0$.

Model 4.—A star formation burst that begins at z_* and has a constant SFR for 1 Gyr.

Model 5.—A star formation burst that begins at z_* and has a constant SFR for 4 Gyr.

Model 6.—An initial star formation burst that lasts for 4 Gyr with a constant SFR and converts 50% of the total mass into stars, followed by another stage of a lower constant SFR that produces the remaining 50% of the stars (“stepwise SFR”).

For all the cases we normalize the SFR in such a way that the total amount of matter converted into stars is equal to the integral over time of equation (2). The overall normalization is of no real significance, however, since we are interested in the qualitative behavior of SNe counts.

The computations provide us with information on the behavior of SNe rates with redshift for different star formation histories. The results provide insights into the understanding the SNe histories in galaxies of different morphological types, which show a wide variety of star formation patterns both along the Hubble sequence and within particular classes (e.g., Sandage 1986; Hodge 1989; Kennicutt, Tamblyn, & Congdon 1994; Kennicutt 1998). Even among the Local Group dwarf galaxies one encounters very different star formation histories, including early bursts, almost constant SFR, and stepwise ones (e.g., Mateo 1998).

Figures 5 and 6 present the number counts of SNe Ia per unit Δz and the cumulative rates of events $n(<z)$ for the above models. The results can be summarized as follows.

1. Models 3 and 4, with initial starbursts of different durations $\Delta\tau$, clearly predict an abrupt decline in the SNe II rate when moving from z_* to lower redshifts, reflecting the cessation of star formation. The redshift of this sharp decline in the rate indicates (for given cosmological parameters) the value of $\Delta\tau$. It also depends of course on z_* . The behavior of SNe Ia from ELDs in systems with He donors (He-ELD) and Chandrasekhar mass SNe in systems

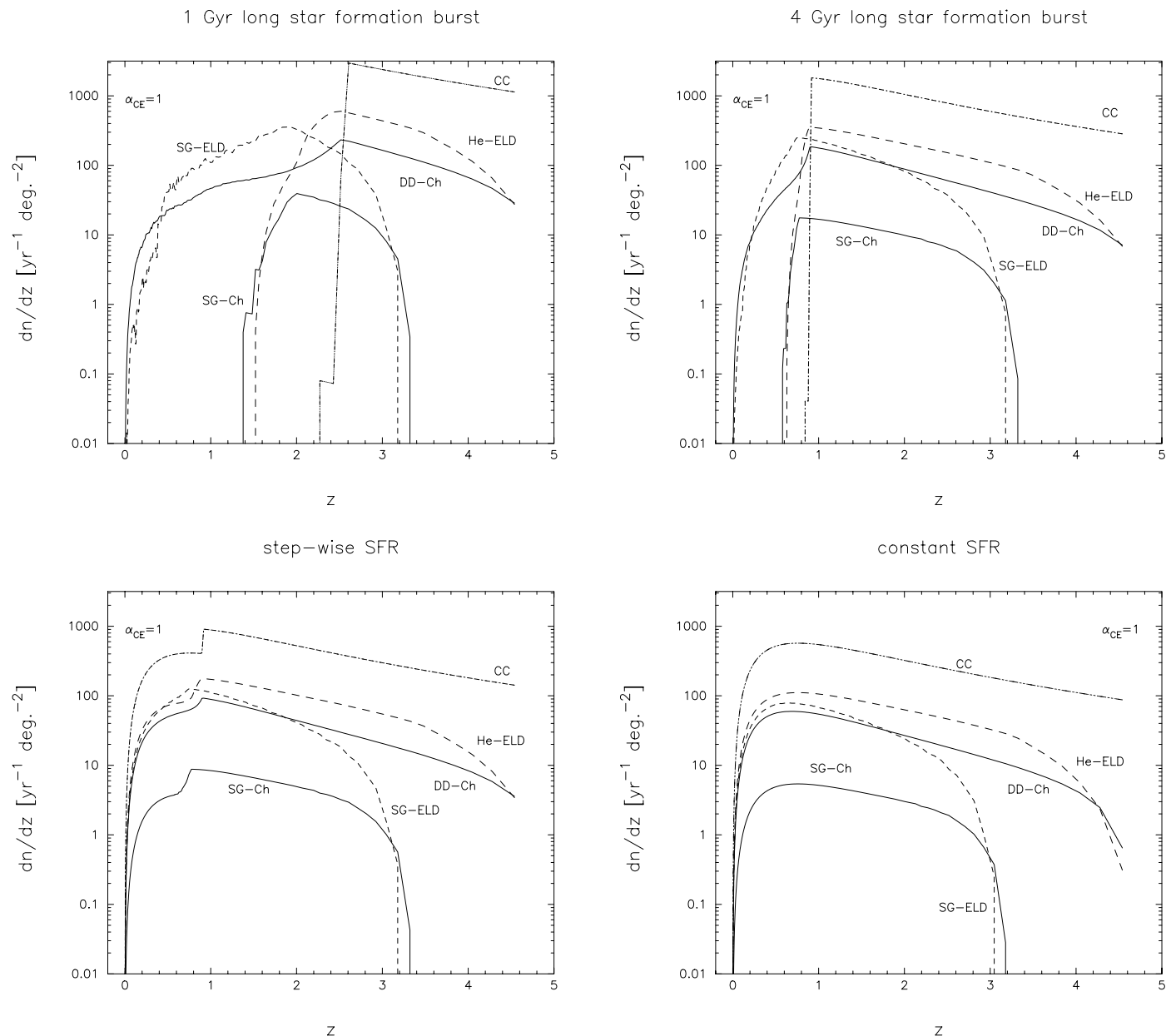


FIG. 5.—Number counts of SNe per unit Δz vs. redshift for different channels of explosive events and different parameterized star formation histories (models 3–6). Notations as in Fig. 2.

with subgiant donors (SG-CH) shows a similar decline, but shifted to a lower z and less abrupt. For stellar populations with strong initial star formation bursts this means that, if He-ELD and SG-Ch SNe Ia were the only mechanisms for SNe Ia, then as one advances to higher redshifts, first the rate of SNe Ia and then the rate of SNe II would rapidly rise. In the case of SG-Ch SNe Ia the rate would rapidly decline at $z \sim 3.3$. Such a behavior of the rates of SNe Ia in E-S0 galaxies would provide evidence supporting the SG-Ch mechanism for SNe Ia.

2. Strong initial peaks in the SFR followed by a variation of the SFR on a short timescale manifest themselves in changes in d^2n/dz^2 for SNe Ia. These changes are delayed (to lower redshifts) compared to the decrease in the SNe II rates.

3. SNe Ia from the mergers of double degenerates (DD-

Ch) are the only types of events that may show up close to z_* and that continue to $z = 0$ irrespective of the star formation mode.

4. Although SNe Ia from ELDs in subgiant systems (SG-ELD) start to explode only at $z \approx 3$, in the constant SFR and stepwise SFR models, at $z \lesssim 2$ the distribution of their number counts versus z becomes very similar to the one from double degenerates (DD-Ch) both in morphology and in amplitude. These SNe, however, follow the variations in the SFR slightly slower. These two Types of SNe Ia are the only events that may be present at low z even if the star formation process ceased long ago (see, however, § 5).

5. SNe Ia from collapses of Chandrasekhar mass white dwarfs in subgiant systems (SG-Ch) may be observed only if the star formation still continues or ceased less than ≈ 2 Gyr ago (see, however, § 5). The same is true for SNe from

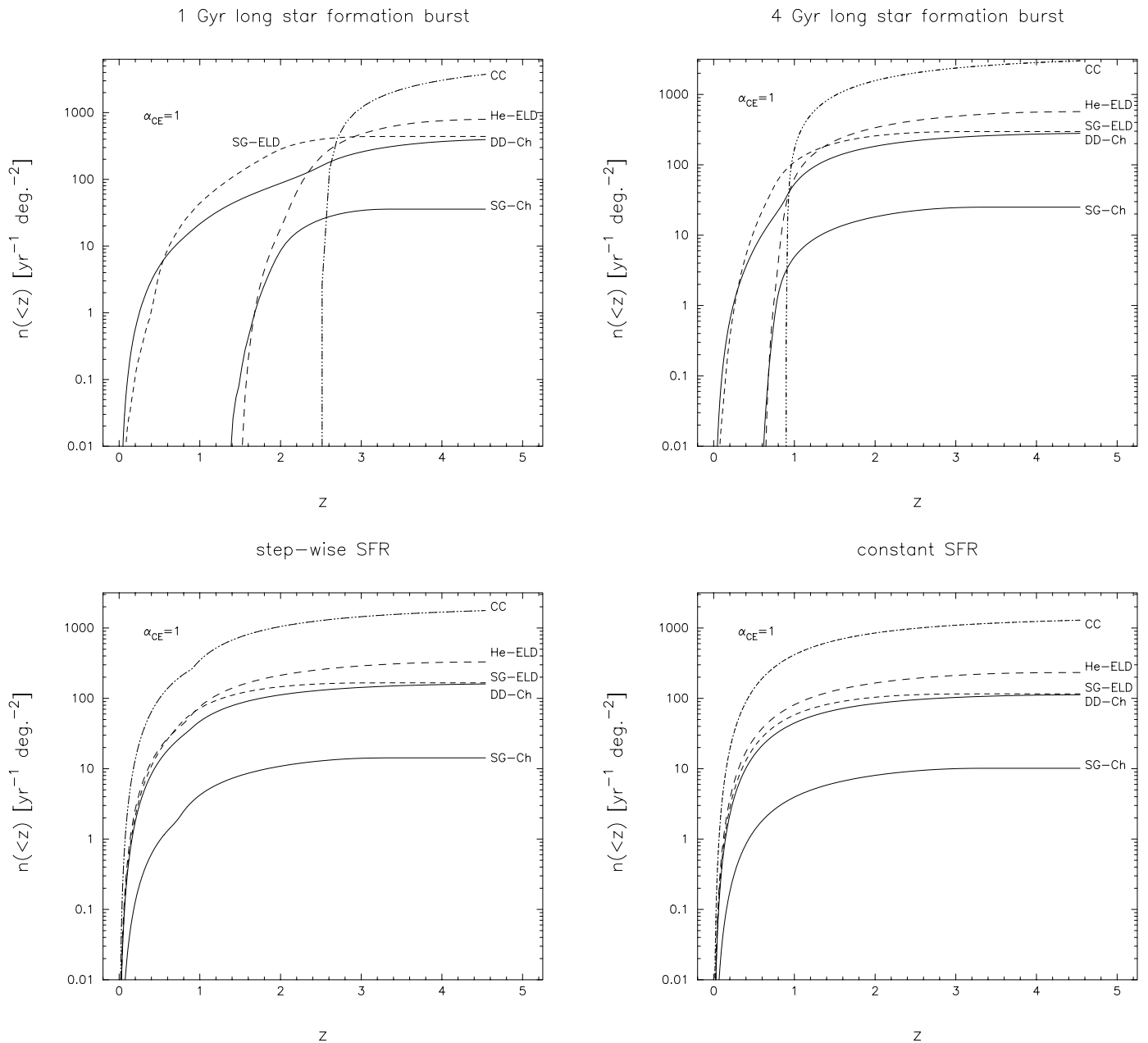


FIG. 6.—Cumulative counts of SNe below a given redshift z for different channels of explosive events in models 3–6. Notations as in Fig. 2.

ELDs in systems with nondegenerate donors (He-ELD). A fast decline of the SNe Ia rate shortly after (at lower z) the decline of the SNe II rate would indicate that either He-ELD or SG-Ch occur.

6. In the case of a SFR that was almost constant during the past several Gyr there is no decline in the SNe Ia/SNe II ratio between $z = 0$ and 1.

7. The difference between the behavior of dn/dz for a constant-rate and for stepwise SFR models is not significant. This means that only a very significant increase in the SFR toward high z (like in Model 2) may be reflected in the behavior of the differential SNe counts. On the other hand, a rapid decline in the SFR beyond a certain redshift (like in Model 2) can be detected easily.

8. The counts of dn/dz in the redshift range $z \lesssim 0.2$ –0.4 can hardly provide any information about the SFR since they are dominated by the increase of the comoving volume.

5. DISCUSSION AND CONCLUSIONS

Since observations of SNe Ia are now being used as one of the main methods for the determination of cosmological parameters, the importance of identifying the progenitors of SNe Ia cannot be overemphasized. We have shown that different progenitor models result in different SNe Ia rates (or different ratios of frequencies of SNe Ia to those resulting from massive stars) as a function of redshift. One key difference, for example, is in the fact that in all the models that involve relatively long delays between the formation of the system and the SN event (e.g., models with subgiant donors), the ratio $R(\text{SNe Ia})/R(\text{SNe II, Ia, Ic})$ decreases essentially to zero at $z \gtrsim 3$ (Fig. 7). Thus, future observations with *NGST* will in principle be able to determine the viability of such progenitor models on the basis of the frequencies of SNe Ia at high redshifts.

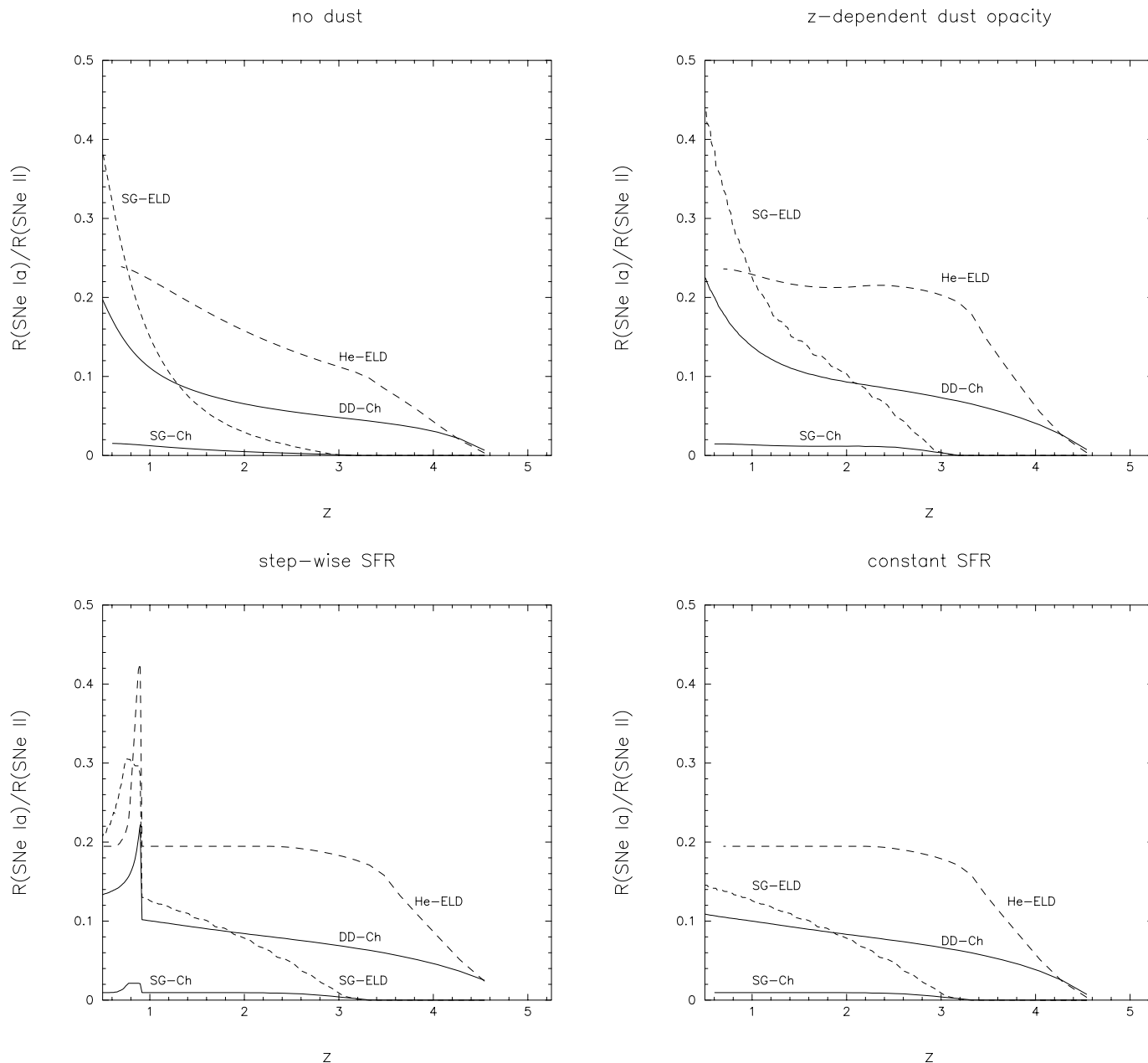


FIG. 7.—Ratios of the rates of different possible SNe channels to core-collapse SNe, for different assumptions on the dust and the SFR (see text). Notations as in Fig. 2.

Probably the most important question that needs to be answered is the following: assuming that two (or more) different classes of progenitors may produce SNe Ia, is it possible that the rate of SNe Ia is entirely dominated by one class at low redshifts ($z < 0.5$) and by another at higher redshifts ($0.5 \lesssim z \lesssim 1.2$)? Clearly, if this were the case, then the suggestion of a cosmological constant would have to be reexamined (SNe Ia at the higher z only need to be systematically dimmer by ~ 0.25 mag to mimic the existence of a cosmological constant). An examination of the qualitative behavior of the rates in Figure 7 reveals that *in principle*, the rate at low redshifts could be dominated by ELDs, while the rate at higher redshifts by coalescing degenerates. However, if ELDs produce SNe Ia at all, these are probably of the underluminous variety (such as SN 1991bg; e.g., Nugent et al. 1997; Livio 1999; Ruiz-Lapuente et al. 1997). Therefore,

a division of this type would produce exactly the opposite effect to the one required to explain away the need for a cosmological constant (the high-redshift ones would be brighter). A second possibility is that the rate of SNe Ia resulting from the accumulation of M_{Ch} in systems with giant or subgiant components (SG-Ch) has been underestimated. This is in fact a very likely possibility. A number of potential ways have been suggested to increase the frequency of SNe Ia of this class (e.g., Hachisu, Kato & Nomoto 1999). These ways include (1) mass stripping from the (sub-)giant companion by the strong wind from the white dwarf (this has the effect of increasing the range of mass ratios that result in stable mass transfer) and (2) an efficient angular momentum removal by the stellar wind in wide systems (where the wind velocity and orbital velocity are comparable; this increases the range of binary separa-

tions with result in interaction). While large uncertainties plague both of these suggestions (see Livio 1999 for a discussion), it is definitely possible that some physical processes that have not yet been properly included in the population synthesis calculations will result in a significant increase in the rates from the channel with giant or subgiant companions. This means that in principle, the curve describing the SG-Ch channel (subgiant donor) in Figure 7 (with the z -dependent dust opacity), may have to be shifted upward (essentially parallel to itself, because of the involved delays). The curve could be shifted just enough for double degenerates to dominate at redshifts $z \lesssim 0.5$, while SG-Ch dominate at $z \gtrsim 0.5$. The question is now, could such a dominance shift be responsible for the apparent need for a cosmological constant? The answer is that this is definitely possible *in principle*. In particular, it has recently been suggested that the fiducial risetime of nearby SNe Ia is ~ 2.5 days longer than that of high-redshift SNe Ia (Riess et al. 1999a; 1999b). It is far from clear, though, whether such a change in the rise time (if real) could be attributed to different progenitor classes or to other evolutionary effects. One possibility could be that because SNe Ia resulting from double degenerates (if they indeed occur; Livio 1999) may have different surface compositions from those resulting from subgiant donors, this could affect the risetime. We would like to note, however, that we find the possibility of one progenitor class dominating at low redshifts and

another at high redshifts rather *unlikely* (see also Livio 1999). The reason is very simple. As Figure 7 shows, even if the SG curve were to be shifted upward, the result would be that the local (low- z) sample would have to contain a significant fraction of the SNe resulting from the SG channel. Therefore, unless SNe Ia from the SG channel conspire to look identical to those from double degenerates at low z , but different at high z , this would result in a *much less homogeneous* local sample than the observed one (which has 80%–90% of all SNe Ia being nearly identical “Branch normals”; e.g., Branch 1998 and references therein). Consequently, it appears that the observational indication of the existence of a cosmological constant cannot be the result of us being “fooled” by different progenitor classes (this does not exclude the possibility of other evolutionary effects).

Finally, our models indicate that a careful determination of the rates of SNe Ia as a function of redshift can place significant constraints on the cosmic star formation history, and on the significance of dust obscuration.

This work was supported by the Russian Foundation for Basic Research grant No. 96-02-16351. L. R. Y. acknowledges the hospitality of the Space Telescope Science Institute. M. L. acknowledges support from NASA grant NAG5-6857. We acknowledge helpful discussions with N. Chugaj, M. Sazhin, and A. Tutukov, and useful comments by D. Branch.

REFERENCES

- Blain, A. W., Smail, I., Ivison, R. J., & Kneib, J.-P. 1999, MNRAS, 302, 632
 Branch, D. 1998, ARA&A, 36, 17
 Branch, D., Livio, M., Yungelson, L., Boffi, F., & Baron, E. 1995, PASP, 107, 717
 Branch, D., Romanishin, W., & Baron, E. 1996, ApJ, 465, 73
 Calzetti, D., & Heckman, T. M. 1999, ApJ, 519, 27
 Canal, R., Ruiz-Lapuente, P., & Burkert, A. 1996, ApJ, 456, L101
 Cappellaro, E., Turatto, M., Tsvetkov, D., Yu., Bartunov, O. S., Pollas, C., Evans, R., & Hamuy, M. 1997, A&A, 322, 431
 Cassisi, S., Iben, I., & Tornambè, A. 1998, ApJ, 496, 376
 Dahlén, T., & Fransson, C. 1999, A&A, 350, 349
 Ferguson, H. C. 1998, preprint (astro-ph/9801058)
 Hachisu, I., Kato, M., & Nomoto, K. 1996, ApJ, 470, L97 (HK N)
 ———. 1999, ApJ, 522, 487
 Hamuy, M., et al. 1996, AJ, 112, 2398
 Hodge, P. W., 1989, ARA&A, 27, 139
 Höflich, P., & Khokhlov, A. 1996, ApJ, 457, 500
 Hu, E. M., Cowie, L. L., & McMahon, R. G. 1998, ApJ, 502, L99
 Hughes, D. H., et al. 1998, Nature, 394, 241
 Iben, I., Jr. 1997, in Thermonuclear Supernovae, ed. P. Ruiz-Lapuente, R. Canal, & J. Isern (Dordrecht: Kluwer), 111
 Jørgensen, H. E., Lipunov, V. M., Panchenko, I. E., Postnov, K. A., & Prokhorov, M. E. 1997, ApJ, 486, 110
 Kato, M., Saio, H., & Hachisu, I. 1989, ApJ, 340, 509
 Kennicutt, R. C. 1998, ARA&A, 36, 189
 Kennicutt, R. C., Tamblyn, P., & Congdon, C. W. 1994, ApJ, 435, 22
 Kobayashi, C., Tsujimoto, T., Nomoto, K., Hachisu, I., & Kato, M. 1998, preprint (astro-ph/9806335)
 Livio, M. 1999, in Supernovae Type Ia: Theory and Cosmology, ed. J. C. Niemeyer & J. W. Truran (Cambridge: CUP), in press
 Madau, P. 1997, in The Hubble Deep Field, ed. M. Livio, S. M. Fall, & P. Madau (Cambridge: Cambridge Univ. Press), 200
 Madau, P. 1998a, in The Next Generation Space Telescope: Science Drivers and Technological Challenges, 34th Liège Astrophysics Colloq., in press
 Madau, P. 1998b, preprint (astro-ph/9801005)
 Madau, P., Della Valle, M., & Panagia, N. 1998, MNRAS, 297, L17 (MDVP98)
 Madau, P., Pozzetti, L., & Dickinson, A. 1998, ApJ, 498, 106
 Mateo, M. 1998, ARA&A, 36, 435
 Nugent, P., Baron, E., Branch, D., Fisher, A., & Hanschildt, P. H. 1997, ApJ, 485, 812
 Perlmutter, S., et al. 1999, ApJ, 517, 565
 Pettini, M., et al. 1998, preprint (astro-ph/9806219)
 Riess, A. G., et al. 1998, AJ, 116, 1009
 Riess, A. G., Filippenko, A. V., Li, W., Treffers, R. R., Schmidt, B. P., Qiu, Y., Hu, J., Armstrong, M., Faranda, C., & Thouvenot, E. 1999a, preprint (astro-ph/9907037)
 Riess, A. G., Filippenko, A. V., Li, W., & Schmidt, B. 1999b, preprint (astro-ph/9907038)
 Ruiz-Lapuente, P., Burkert, A., & Canal, R. 1995, ApJ, 447, L69
 Ruiz-Lapuente, P., & Canal, R. 1998, ApJ, 497, L57
 Ruiz-Lapuente, P., Canal, R., & Burkert, A. 1997, in Thermonuclear Supernovae, ed. P. Ruiz-Lapuente, R. Canal, & J. Isern (Dordrecht: Kluwer), 205
 Sadat, R., Blanchard, A., Guiderdoni, B., Silk, J. 1998, A&A, 331, L69
 Sandage, A. 1986, A&A, 161, 89
 Steidel, C. C., Adelberger, K. L., Giavalisco, M., Dickinson, M., & Pettini, M. 1999, ApJ, 519, 1
 Tutukov, A., Yungelson, L., & Iben, I. Jr. 1992, ApJ, 386, 197
 Umeda, H., Nomoto, K., Yamaoka, H., Wanajo, S. 1999, ApJ, 513, 861
 Yungelson, L., & Livio, M. 1998, ApJ, 497, 168
 Yungelson, L., & Tutukov, A. 1997, in Advances in Stellar Evolution, ed. R. T. Rood, & A. Renzini (Cambridge: Cambridge Univ. Press), 237
 Yungelson, L., Livio, M., Tutukov, A., & Kenyon, S. J. 1995, ApJ, 447, 656
 Zeldovich, Ya. B., & Novikov, I. D. 1983, The Structure and Evolution of the Universe (Chicago: Univ. of Chicago Press)